Peer-reviewed version available at Gels 2018, 4, 73; doi:10.3390/gels4030073

Article

A Comparative Study of a 3D Bioprinted Gelatin-Based *Lattice* and *Rectangular-Sheet* Structures

Shweta Anil Kumar[1], Nishat Tasnim[1], Erick Dominguez[1], Shane C. Allen[2], Laura Suggs[2], Yoshihiro Ito[3,4], Binata Joddar[1,5*]

[1] Inspired Materials & Stem-Cell Based Tissue Engineering Laboratory (IMSTEL), Department of Metallurgical, Materials and Biomedical Engineering, University of Texas at El Paso, 500 W University Avenue, El Paso, TX 79968, USA.
[2] Department of Biomedical Engineering, The University of Texas at Austin, Austin, Texas 78712, USA.
[3] Nano Medical Engineering Laboratory, RIKEN, 2-1 Hirosawa, Wako, Saitama 351-0198, Japan.
[4] Emergent Bioengineering Materials Research Team, RIKEN Center for Emergent Matter Science, 2-1 Hirosawa, Wako, Saitama 351-0198, Japan.
[5] Border Biomedical Research Center, University of Texas at El Paso, 500 W University Avenue, El Paso, TX 79968, USA
* Correspondence: Binata Joddar; bjoddar@utep.edu; Phone: (915) 747-8456, Fax: (915) 747-8036.

Abstract: 3D bioprinting holds great promise in the field of regenerative medicine as it can create complex structures in a layer-by-layer manner using cell-laden bioinks, making it possible to imitate native tissues. Current bioinks lack both the high printability and the biocompatibility required in this respect. Hence, the development of bioinks that are capable of both properties is needed. In our previous study, a furfuryl-gelatin based bioink, crosslinkable by visible light, was used for creating mouse mesenchymal stem cell-laden structures with high fidelity. In this study, *lattice* mesh geometries were printed in a comparative study to test against the properties of a traditional *rectangular-sheet*. After 3D printing and crosslinking, both structures were analysed for swelling and rheological properties, and their porosity estimated using scanning electron microscopy. Results showed that the lattice structure was relatively more porous but sturdy and exhibited a lower degradation rate compared to the rectangular-sheet. Further, the lattice allowed encapsulation of a greater number of cells, allowing them to proliferate to a greater extent compared to the rectangular-sheet that retained a lesser number of cells initially. All of these results collectively affirmed that the lattice poses as a superior scaffold design for tissue engineering applications.

Keywords: hydrogels; cardiac patches; 3D bioprinting; furfuryl-gelatin; lattice

1. Introduction

The creation of cell patterns within specific spaces with the retention of their cell function and vitality, through 3D bioprinting, is a method that can be dated back to the 1990s [1]. This technique, with its vast potential and ceaseless possibilities, can bring about path-breaking changes in the field of regenerative medicine and therapeutics by generating complex tissues and organs that can be implanted in-vivo [1]. 3D bioprinting employs a 'bioprinter' which uses 'bioink' that can exhibit the characteristics of an extracellular matrix environment and facilitate cell adhesion, proliferation and differentiation [2- 5]. Bioinks usually have the cells suspended in a hydrogel-like mixture and loaded within extrusion devices such as syringes prior to printing [6]. After printing, the structural fidelity of the printed shape is retained by secondary crosslinking mechanisms [7]. Traditional bioinks used for bioprinting do not generally possess high fidelity and biocompatibility, which fails to reproduce the complexity in biological organs or tissues. So, in a recent study, we optimized the properties of a visible light crosslinkable gelatin-based bioink and successfully printed bilayer rectangular-sheet

Peer-reviewed version available at Gels 2018, 4, 73; doi:10.3390/gels4030073

structures infused with C2C12 myoblasts and STO fibroblasts [7]. The furfuryl-gelatin (f-gelatin) crosslinks through visible-light irradiation, where O2 changes to $^1O_2$ (singlet-oxygen) when the Rose Bengal dye acquires energy from visible-light [7]. The formation of singlet-oxygen leads to the formation of a stable cross-linked f-gelatin structure after bioprinting and deposition [7]. These bioprinted cell-sheets exhibited high fidelity during sustained in vitro culture and the encapsulated cells retained viability and exhibited heterocellular coupling [7]. However, the study did not provide any scope to assess the ability of this gelatin-based bioink to create complex structures such as a lattice [8], which may serve as an enhanced physical scaffold and provide microarchitectural cues necessary for mimicking the native architecture of the myocardium [9]. This subsequent study explored the feasibility of 3D bioprinting a lattice structure using the same f-gelatin based bioink and compared it with the rectangular-sheet structure from the prior study by careful considerations of factors like structural fidelity, rheological properties, porosity and cytocompatibility. We hypothesised that the experiments performed as a part of this study would help us to observe considerable differences between the two structures, i.e., lattice and rectangle and also open up the possibility of significantly enhancing the design of a 3D bioprinted construct for engineering cardiac tissue-on-a-chip, using bioprinting.

2. Results and Discussion

Comparison of morphology between the two rectangular-sheet structures made using either pluronic or f-gelatin based bioink revealed the following results. These two rectangular-sheet structures appeared similar in morphology and dimensions (Figure 1 B (II) and (III)). On the other hand, the lattice structures fabricated using either pluronic or f-gelatin based bioink revealed significant differences (Figure 1 A (II) and (III)). The stereolithography (stl) designs used for printing are depicted in Figure 1 A(I) and B(I), respectively. The pluronic lattice structure retained the structural complexity and fidelity of the lattice greatly, compared with the f-gelatin based structure (Figure 1 A (II) and (III)).

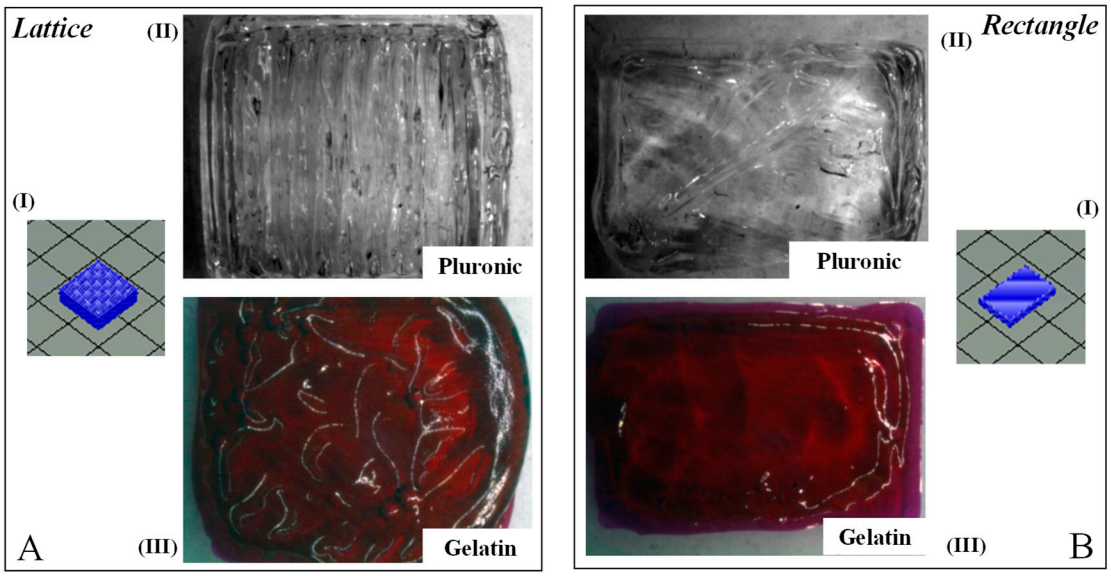

Figure 1. Gross Morphology of lattice and rectangular sheet structures printed using pluronic and gelatin. A(I) and B(I) depict the stl. file image for the lattice and rectangular structures respectively. A(II) and B(II) represent the *en-face* images for the same printed using Pluronic F-127. A(III) and B(III) are representations of the *en-face* images for lattice and rectangular patterns printed using the f-gelatin based bioink.

Similarly, scanning electron microscopy (SEM) en-face images of both, lattice and rectangular-sheet revealed significant differences in lattice structures only, casted using pluronic and f-gelatin based bioinks (Figure 2 A (I) and (II). On the other hand, the rectangular-sheet

Peer-reviewed version available at Gels 2018, 4, 73; doi:10.3390/gels4030073

structures made using either pluronic (Figure 2 B (I)) or f-gelatin (Figure 2 B (II)) exhibited structural resemblance.

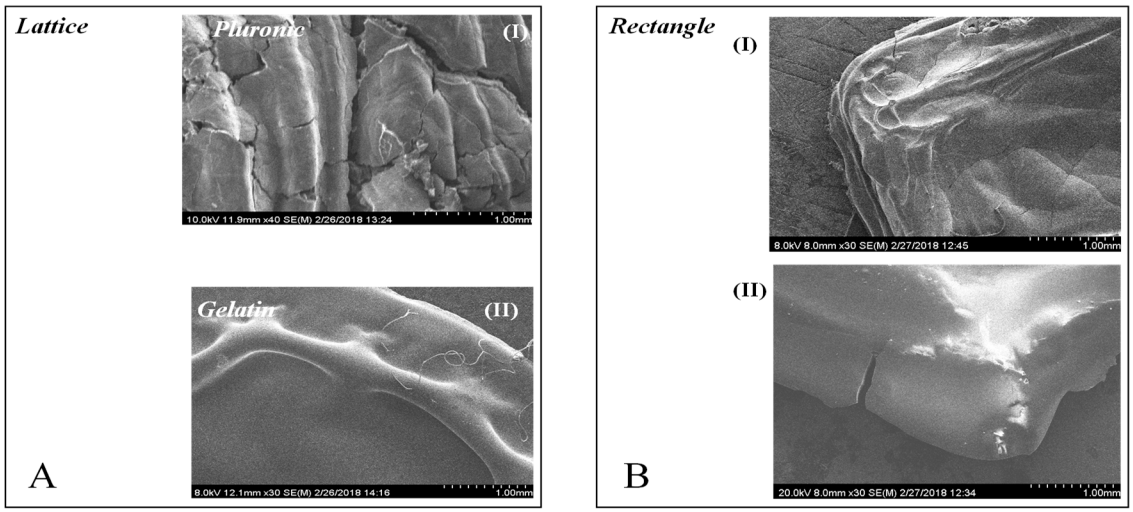

Figure 2. Representative SEM surface images of lattice and rectangular-sheet structures deposited using pluronic and gelatin. A(I) and A(II) show the en-face images for the lattice structures printed with Pluronic-F127 and the f-gelatin based bioink, respectively. B(I) and B(II) depict the en-face images for the rectangular structures printed using the same materials, respectively.

The SEM cross-sectional image of the gelatin lattice revealed a highly organized, striated, patterned and networked structure (Figure 3) in comparison to the loosely networked and largely porous rectangular-sheet cross-section SEM, as reported in our previous study [7]. Porosity and pore-size are crucial to ensure cell colonization of the scaffold, deposited using bioprinting. Likewise, SEM micrographs (Figure 3) showed a homogeneous distribution of equal sized pores within the entire area scanned and imaged (Figure 3).

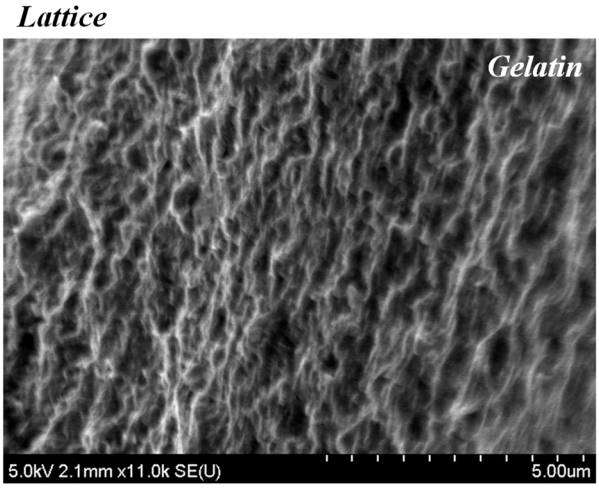

Figure 3. A representative SEM cross-section image of a gelatin lattice structure that was acquired in order to determine the apparent porosity and average pore size. The cross-sectional SEM image for the rectangular-sheet structure printed using f-gelatin was previously reported [7].

Furthermore, the cross-section SEM image also showed well-interconnected pores with a mean value of 1 μm (Figure 3). This was significantly lesser compared to the average pore size of the rectangular-sheet structures, as reported in our previous study [7]. The average apparent porosity of this lattice structure was estimated to be about 50% compared to 21% for the rectangular-sheet [7]. Results led us to conclude that although the mean pore size was significantly reduced by printing in

Peer-reviewed version available at Gels 2018, 4, 73; doi:10.3390/gels4030073

the form of a lattice, the inherent design of the lattice allowed pores to be of similar size and to be homogenously distributed throughout the entire structure, compared with the rectangular-sheet [7].

The swelling kinetics and behaviour of bioprinted lattice and rectangular crosslinked hydrogels is depicted in Figure 4. For all samples tested, the maximum swelling was observed at 24 hrs, as reported in our previous study [7]. After 24 hrs of incubation, the structures seem to degrade slightly as evidenced by 48 hr (Figure 4A). However, the lattice structure seemed to have reached an equilibrium point after 48 hr as it did not exhibit any further degradation beyond 48 hr, when analysed at 72 hr (Figure 4A). On the other hand, the rectangular-sheet continued to degrade beyond 48 hr, when analysed at 72 hr. These results enabled us to conclude that the lattice posed a more stable structure compared with the rectangular-sheet (Figure 4A). Although data reported was from 3 days of observation and analysis, the stored gels did not degrade until 6 days in culture following this observation.

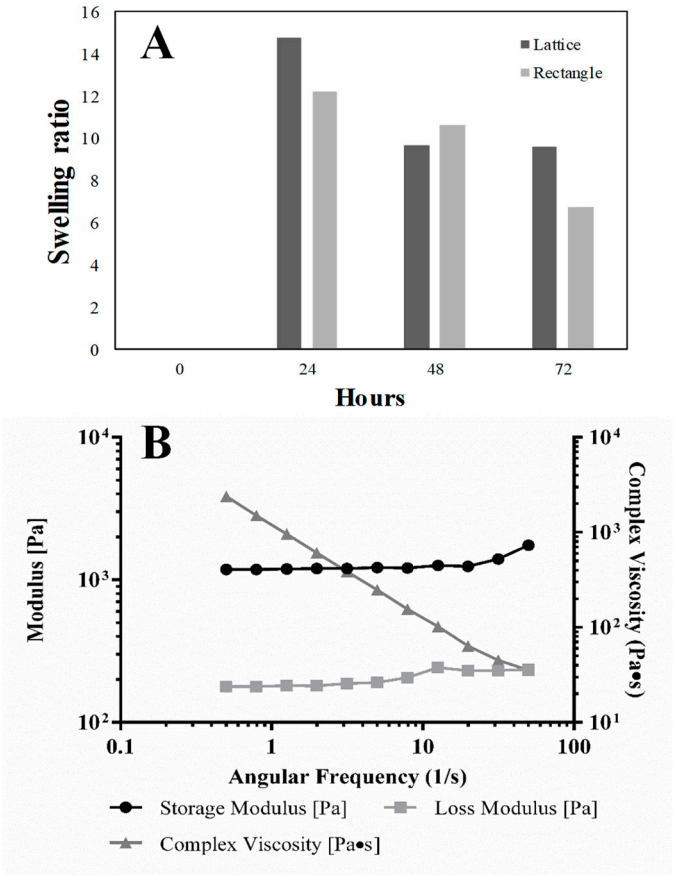

Figure 4. (A) Swelling analysis for both the f-gelatin based, lattice and rectangular-sheets over a period of 3 days after being subjected to visible light crosslinking. (B) Rheology analysis of f-gelatin based lattice structures, obtained from a disc-shaped (8 mm) sample.

From the rheometric analysis, it was established that the strain and frequency range were in the linear viscoelastic range of the gels by amplitude and frequency sweeps (Figure 4B). The crosslinked gels exhibited an elastic modulus of 5.5 ± 2.4 kPa and complex viscosity of 920 ± 400 Pa.s, both of which were significantly higher, ~5 times compared to the respective values of the rectangular sheet structure [7]. These results implied that although the bioink material composition and the crosslinking mechanism was unaltered, the lattice geometry influenced the mechanical properties of

Peer-reviewed version available at Gels 2018, 4, 73; doi:10.3390/gels4030073

the printed structure. However, the larger error is due to the fact that the lattice structures were more difficult to measure with shear.

Live/Dead assay results showed the evidence of fewer dead cells compared to a greater number of live cells, after bioprinting and crosslinking of the printed structure (Figure 5). The number of live cells was significantly more ($p=0.03$) at 22 ± 5 per unit area (12 X 10^4 sq. microns) compared to the number of estimated dead cells per unit area (6 ± 2). This data was in the range of results shown by others during cell bioprinting via extrusion methods [10].

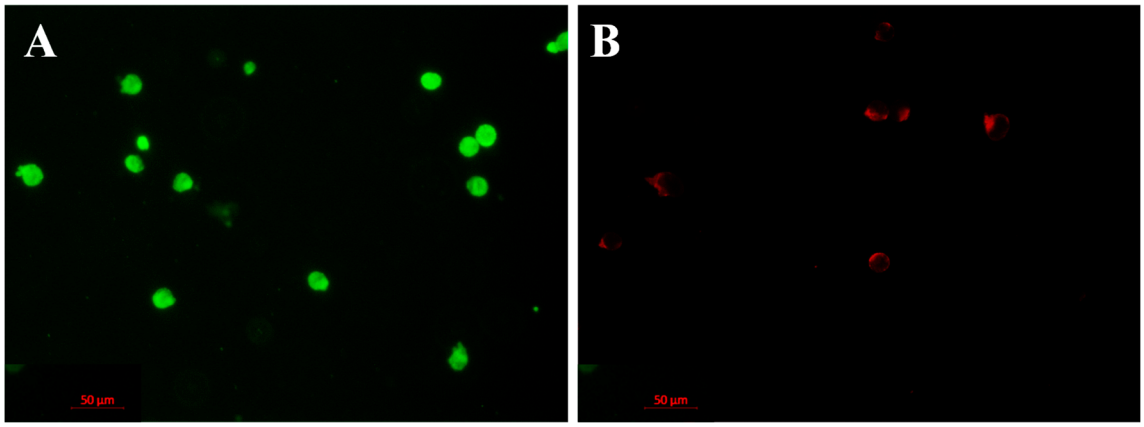

Figure 5. Live/Dead assay performed 15 min after printing and crosslinking. Shown in (A) are calcein stained live cells and in (B) are ethidium homodimer stained dead cells, respectively.

To estimate cell proliferation in the bioprinted lattice and rectangular-sheet structures, the cells were pre-stained using Cell Trace Violet (CTV), proliferation kit (Invitrogen, Carlsbad, CA, USA) and subjected to Flow Cytometry (FACS) analysis. Results from FACS analysis showed that from 24- till 72 hr of culture, cells cultured within the lattice showed enhanced proliferation compared to the rectangular-sheet (Figure 6). This is because the Gated X-A mean was significantly reduced in its value from 24- till 72-hr in cells cultured within the lattice (1.23 versus 0.44 respectively) compared to the rectangle which did not reveal significant differences from 24- till 72-hr (0.60 versus 0.62 respectively). Further, the occurrence of multiple peaks (Figure 6) confirmed the presence of consecutive proliferating generations of cells, in the bioprinted constructs. The positive controls consisting of CTV stained cells cultured on plastic for 24- and 72-hr also showed enhanced dye dilution and cell generations from 24- till 72-hr as indicated by their Gated X-A mean values (Supplementary Figure 1). In summary, the lattice structure, allowed cells to connect and communicate better resulting in higher cell growth indicated by the greater extent of dye dilution, compared to the rectangular-sheet structure. These results were cross verified from absolute cell counts, as described. For the 3D printed constructs, 2 X 10^5 cells/ml were used for cell encapsulation. Since the lattice had a larger volume (1.5 cm × 1.5 cm × 1 mm) than the rectangular sheet (1.5 cm × 1 cm × 1 mm), more cells could be entrapped within the lattice compared to the rectangle when analysed after 24 hours at which time, the lattice revealed a cell density of 4.2 X 10^5 cells/ml compared to the rectangular sheet which had 2.4 X 10^5 cells/ml. After 72 hours, cells in both samples had proliferated about ~4 times compared to initial cell seeding density. Representative images of samples at specific time points, at 24- and at 72-hours are depicted in Supplementary Figure 2. The value of Gated X-A mean usually refers to the intensity of the dye used for cell tracking and proliferation [11]. The principle of use governing the application of the dye, CTV to track cell proliferation is based on an underlying concept of dye dilution which allows several generations of cells to be analysed using just one-time staining of the cells, prior to culture [11]. As the cells proliferate, the dye intensity gets diluted with increasing generations of cells produced within the same culture. So, a higher value of the Gated X-A mean indicates lesser dye dilution and generations of cells, and a lower value indicates

Peer-reviewed version available at Gels 2018, 4, 73; doi:10.3390/gels4030073

enhanced dye dilution and an increase in the generations of cells, respectively. Thus, the use of dye dilution assays on asynchronously growing cell lines is a potentially powerful method for tracking cell proliferation [12]. In our previously published study [7], the CTV dye was used at a 1:1000 dilution and so the proportional decrease in the intensity of the dye with enhancing cell populations could not be detected. So, in this study, we chose to apply a 1:5000 dilutions to detect the proportional decrease in the intensity of the dye, expressed by generations of proliferating cells.

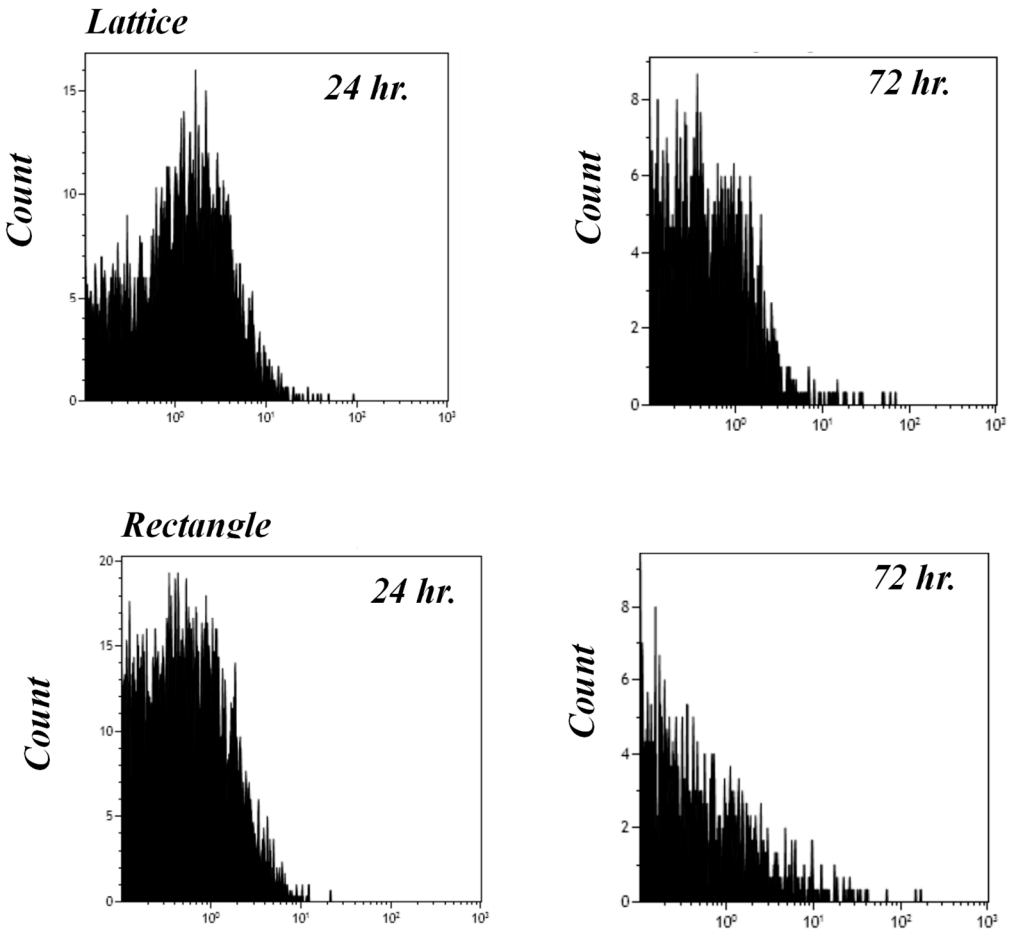

Gated X-A mean	For Lattice	For Rectangle
24 hours	1.23	0.60
72 hours	0.44	0.62

Figure 6. FACS analysis to show cell proliferation and biocompatibility of the printed and crosslinked, lattice and rectangular-sheet structures, respectively. Cells pre-stained with cell trace violet (CTV) were cultured up to 24- and 72-hr. within printed constructs respectively. Gated X-A mean values indicate the average intensity of the dye exhibited during that particular sample run.

SEM images of cells in lattice structures revealed morphologies that were characteristic of healthy, and proliferating cells [13] (Figure 7 A, B). Besides there was also a significant amount of extracellular matrix (pointed using white block arrows) deposited by cells, noted in all representative images (Figure 7 A, B). These results implied that the lattice is a favourable scaffold design permissive towards cell growth and proliferation, owing to its macro-porosity (Supplementary Figure 3).

To summarize the results from this study, the lattice structure appeared to present itself as a more stable scaffold with both structural rigidity, optimal porosity and well-connected pores which allowed the cells cultured within to proliferate more, compared to the rectangular-sheet structure.

This study revealed fundamental differences in two dissimilar, chemically cross-linked soft structures fabricated using the same bioink.

The lattice allows more bioink volume to be deposited, thereby allowing a greater number of cells to be encapsulated within the printed structure. Most importantly, the lattice structure allows cells to communicate better eventually resulting in better cell yields compared to the rectangular-sheet.

Thus, the lattice structure poses as a better choice for a scaffold for creating 3D bioprinted structures for tissue engineering applications. The lattice is a multi-layered structure and in the future, it can be explored as a suitable platform for culturing multiple cell types within the same structure in a layer-by-layer fashion [14].

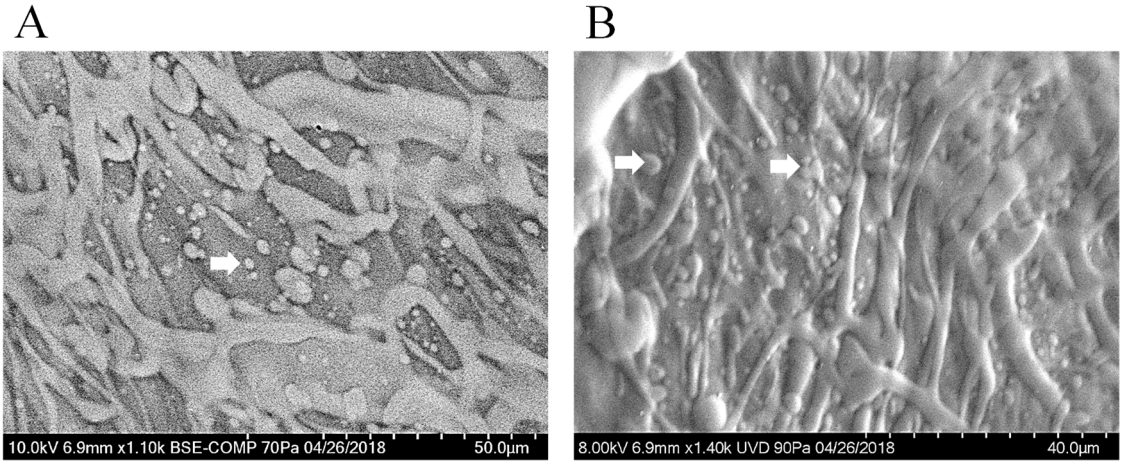

Figure 7. Shown in A and B are characteristic images of mouse MSC printed in lattice structures. Elongated cell morphologies and extensive coverage area by the cells, both confirm the biocompatibility of the lattice design and the bioink used. White arrows point to the extracellular matrix deposited by the cells cultured.

3. Materials and Methods

3.1. Chemicals:

Furfuryl gelatin (f-gelatin), used as a basis for the 'bioink' was synthesized and characterized as described [15, 16]. Hyaluronic Acid Sodium Salt (HA; mol. wt. ~1.5-1.8 x 10E6 Da) was obtained from Sigma-Aldrich (St. Louis, MO, USA). Rose Bengal (RB), a visible light crosslinker, was procured from ThermoFisher Scientific (Waltham, MA, USA). Pluronic F127 was obtained as a 'bioink' from Allevi (formerly Biobots, Philadelphia, PA, USA).

3.2. Cells and growth medium:

Strain C57BL/6 Mouse Mesenchymal Stem Cells (mouse MSC, catalogue #: MUBMX-01001) was used to disperse in the 'bioink' and printed into structures. For their culture, growth and maintenance, Mouse Mesenchymal Stem Cell Growth Medium (complete growth medium, catalogue #: MUXMX-90011) was obtained from Cyagen, Santa Clara, CA, USA. Cells were cultured and passaged according to the manufacturer's recommendations.

3.3. Biofabrication:

For biofabrication, an ALLEVI 2 (formerly the BIOBOT 1, Allevi, Philadelphia, PA, USA) we formulated the 'bioink' and cell mixture as optimized in our previous study, as described [7]. The bioink was made up of a mixture of f-gelatin, HA and RB in quantities mentioned earlier [7, 17, 18]. Briefly, to make 1 ml of bioink, 10 mg of HA and 100 mg of f-gelatin was dissolved in DI water (900 µl, 25°C) and mixed thoroughly by heating in a water bath (37°C, 1 hr) to render the formation of a homogenous viscous mixture. To this, 100 µl of RB (5% w/v) was added for crosslinking after bioprinting. Finally, cells were added to this gel-like mixture, loaded within a 10 ml plastic syringe

Peer-reviewed version available at Gels 2018, 4, 73; doi:10.3390/gels4030073

(BD, Franklin lakes, NJ, USA), fitted with a stainless steel blunt-tip dispensing needle (20G, 0.6 mm diameter, Huaha, Amazon, USA) and extruded using low extrusion pressure in the range of 2.6 - 4.8 psi [7]. Two dissimilar patterns namely, a lattice and a rectangular-sheet [7], were used for printing structures, in 100 mm × 15 mm petri-dishes (ThermoFisher). The dimensions of the lattice were 1.5 cm × 1.5 cm and the rectangular-sheet, 1.5 cm × 1 cm. Both structures were printed up to a thickness of 1 mm. After printing, the structures were exposed to visible light for 2.5 min to facilitate chemical crosslinking (400 nm wavelength at 100% intensity, Intelli-Ray 600, Uvitron International, West Springfield, MA, USA).

As a positive control for structural comparison, pluronic was used to mimic complex structures via bioprinting [4]. For printing, pluronic was maintained at room temperature (25°C) until it freely flowed and then loaded within a 10 ml plastic syringe (BD), fitted with a stainless steel blunt-tip dispensing needle (23G, 0.34 mm diameter) and extruded using high extrusion pressure in the range of 25.9 - 29 psi, following recommendations from Allevi.

3.4. Gross Morphology:

To compare and contrast the overall morphology and identify essential dissimilarities in both, printed lattice and rectangular-sheet structures, digital images of structures printed using f-gelatin and pluronic were acquired using an upright Leica M205C microscope (Leica Microsystems, Buffalo Grove, IL, USA).

3.5. Rheology of bioink:

Rheological characterization was evaluated using a previous standardized approach for the proper analysis of hydrogel rheological properties. For measurement, printed and crosslinked gels (without cells) were pre-swollen in 1X PBS (1 hr, 25°C) before testing and cut out from the lattice and rectangular sheet structures, using a biopsy punch (~1 mm deep, 8 mm diameter). We performed oscillatory shear stress rheometry on these gel samples at 1% strain using a frequency range of 0.5 – 50 Hz on an Anton-Paar MCR101 rheometer (Anton-Paar, Graz, Austria) through an 8-mm parallel plate geometry. The strain and frequency range were examined in the linear viscoelastic range of the gels by frequency sweeps. Elastic modulus was calculated by a previously established formula using complex shear modulus with storage and loss modulus, corresponding to the complex viscosity measured at 1.99 Hz for all samples [7, 19].

3.6. In-vitro culture conditions for the cell-laden constructs:

The cell-laden, bioprinted and crosslinked constructs, both lattice and rectangular-sheets were overlaid with complete growth medium for mouse MSC and cultured in an incubator (37°C, 5% CO_2 and 95% RH) upto 72 hours. During this time, the culture medium was changed by removing the spent medium and by adding fresh growth medium after every 24-hour interval. From our previous study, it was shown that culturing the cell-laden constructs in this manner did not affect cell viability nor proliferation even in the interior parts of the construct, as it was reasonably porous allowing nutrient uptake and oxygenation [7]. Moreover, 3D cell printing has been shown to allow the effective generation of a cell-laden porous architecture that enables for a sufficient supply of cellular nutrition and oxygen [20]. In addition, others have shown that porous 3D cell-printed patches exhibit higher cell viability [20], than their non-3D printed counterparts.

3.7. Live/Dead cytotoxicity assay:

The cytotoxicity assay was performed using a Live/Dead assay kit, to assess the biocompatibility of the f-gelatin bioink and the printing method [21]. Mouse MSC after being subjected to extrusion-based bioprinting and visible light crosslinking were subjected to the Live/Dead assay (after 15 min). First, the cell-laden structures were rinsed with 1X PBS (3 times) and supplemented with pre-warmed complete growth medium for an additional 15 min. Then the growth medium was removed and the samples incubated with pre-warmed cytotoxicity reagent (Marker

Gene Technologies Inc. Live/Dead Cytotoxicity Assay Kit Green/Red Staining). Sufficient amount of the reagent was added to cover the samples during the incubation process, for which the samples were placed back into the incubator for 45 min. After incubation, the samples were washed using 1X PBS and imaged using light and confocal microscopy (ZEISS LSM 700 Confocal, Germany). Acquired images were analysed using Image J (NIH) and the number of live or dead cells per unit area was reported as mean ± stdev.

3.8. Scanning electron microscopy:

The porous texture of the lattice was analysed by scanning electron microscopy (SEM) to ensure that hydrogel retained its structure, after printing and crosslinking. Cross-sectional and en-face and images of the dried-gels prepared using the f-gelatin based bioink were acquired using SEM, following published procedures [7, 13]. For SEM, acellular and cell-laden samples were employed to determine the morphology and porous structure of the hydrogels, and cell behaviour on the scaffolds, respectively.

For sample preparation, lattice structures were printed, dried in a desiccator (Nalgene, Sigma) overnight and visualized using SEM. Prior to SEM imaging, samples were sputter-coated with gold (1 min, Au coating thickness of 5 nm) in a sputter coater (Jeol USA Smart Sputter Coater, JEOL USA, Inc. Peabody, MA).

To calculate the average pore size and porosity of the lattice and rectangular-sheet structures, cross sections were prepared for SEM imaging. As this step required a substantial amount of bioink material, only thick sections for the lattice structure were prepared as the data for the rectangular-sheet structures already exists [7]. For sample preparation, for imaging of the cross-section of a lattice structure printed using the f-gelatin based bioink, the prepared samples were dried in a desiccator, sputter-coated and visualized using SEM (S-4800, Hitachi, Japan). Cross-sectional SEM images obtained were analysed using Image J to determine the average pore size and the apparent porosity (%), respectively. Apparent porosity was calculated by the following formulae (1):

$$App.porosity = \frac{total\ area\ covered\ by\ pores\ (sq.\mu m)}{total\ sample\ area\ of\ the\ cross-section(sq.\mu m)} * 100 \qquad (1)$$

SEM was also done to confirm cell retention, spreading and maintenance of viable cell morphology within the scaffolds in addition to revealing the overall structure of the lattice scaffolds. For en-face imaging of samples with cells, cross-section of one representative specimen from each sample pool were examined using a Hitachi TM-1000 SEM equipped with a backscattered electron detector and operating at an accelerating voltage of 15 kV (Hitachi High-Technologies Europe GmbH, Germany) [22].

3.9. Swelling Behaviour:

The swelling behaviour of the gels was monitored in Dulbecco Modified Eagle's Medium (DMEM, pH = 7, 25°C) for 5 days to study the hydration dynamics of the crosslinked hydrogel structure [7, 13]. Two representative structures of one lattice and one rectangular-sheet each, were printed, crosslinked and stored at -80°C (12 hr) following which the samples were dried overnight in a desiccator. These dried samples were weighed (W0) and then immersed in DMEM and the increased weight due to swelling and water intake, was recorded periodically (Wt) after every 24 hr till 72 hrs. The swelling ratio was calculated using the following equation (2), where Ds was the degree of swelling, W0 and Wt were the weights of the samples in the dry and swollen states respectively [7, 13].

$$Ds = \frac{Wt - W0}{WDs} \qquad (2)$$

3.10. Cell Proliferation:

For estimation of the actual cell numbers in a sample at different time points, lattice structures printed with cells and cultured as described earlier, were carefully rinsed with PBS, overlaid with a generous amount of 0.25% trypsin-EDTA and incubated at 37 °C for 10 min on an orbital shaker (45 rpm). Cells extracted from the first-trypsinization cycle were pelleted by centrifugation, added with other cells that were removed in a second cycle of trypsinization and counted using a haemocytometer throughout the entire culture period after 24- and 48-hr of culture. Absolute cells densities extracted from samples at 24- and 48-hr are reported.

3.11. Flow Cytometry (FACS) analysis:

To estimate cell proliferation in the bioprinted lattice and rectangular-sheet structures, the cells were pre-stained using Cell Trace Violet (CTV), proliferation kit (Invitrogen, Carlsbad, CA, USA) using manufacturer's protocols [7, 13]. Briefly, 1:5000 dilutions were used for the CTV dye in this study, for pre-staining cells. These pre-stained cells were mixed with the bioink (2 x 10^5 cells/ml) and printed into lattice or rectangular-sheets and cultured for 24 hr, and 72 hr respectively (37°C, 5% CO_2). After 24- and 72-hr, cell-gel samples were treated using Trypsin-EDTA (0.25%, phenol red) (ThermoFisher), after which the cells were detached, extracted and processed for flow cytometry (FACS). Extracted cells were fixed and processed further for FACS (Beckman Coulter Gallios Flow Cytometer, Brea, CA, USA) using excitation and emission wavelengths of 405 and 450 nm respectively. Positive controls included pre-stained cells (1 x 10^5 cells/ml) grown on plastic petri dishes for 24 and 72 hrs, respectively. Negative controls included non-stained cells grown on plastic petri dishes for 24 and 72 hours, respectively.

Supplementary Materials: The following are available online at www.mdpi.com/xxx/s1, Figure 1: FACS analysis for controls, Figure 2: Cell laden constructs after 24 and 72 hrs, Figure 3: Fabrication of a lattice structure

Author Contributions: Conceptualization, B.J., S.A.K.; Methodology, B.J., S.A.K.; Software, S.A.K.; Validation, B.J., S.A.K. and E.D.; Formal Analysis, B.J., S.A.K; Investigation, B.J., S.A.K., N.T., E.D., S.C.A.; Resources, B.J., L.S.Y.I..; Data Curation, B.J., S.A.K., E.D.; Writing-Original Draft Preparation, B.J., S.A.K.; Writing-Review & Editing, S.A.K.; Visualization, B.J.; Supervision, B.J.; Project Administration, B.J.; Funding Acquisition, B.J.

Funding: B.J acknowledges NIH BUILD Pilot 8UL1GM118970-02 and NIH 1SC2HL134642-01 for funding support and the NSF-PREM program (DMR 1205302) for materials and supplies. N.T acknowledges the Anita Mochen Loya fellowship at UTEP. The authors also acknowledge the use of the Core Facility at Border Biomedical Research Consortium at UTEP supported by NIH-NIMHD-RCMI Grant No. 2G12MD007592. Research reported in this article was also supported by the National Institute of General Medical Sciences of the National Institutes of Health under Linked Award Numbers RL5GM118969, TL4GM118971, and UL1GM118970.The content is solely the responsibility of the authors and does not necessarily represent the official views of the National Institutes of Health.

Acknowledgments: We acknowledge the technical assistance received from Dr Armando Varela for kindly assisting us with the FACS analysis and the confocal microscopy and Dr David Roberson for his help with the SEM.

Conflicts of Interest: The authors declare no conflict of interest.

References

1. Murphy S. V. and A. Atala. 3D bioprinting of tissues and organs. Nature biotechnology 32: 773-785, 2014.
2. Begum J., W. Day, C. Henderson, S. Purewal, J. Cerveira, H. Summers, P. Rees, D. Davies and A. Filby. A method for evaluating the use of fluorescent dyes to track proliferation in cell lines by dye dilution. Cytometry Part A 83: 1085-1095, 2013.
3. Bigi A., G. Cojazzi, S. Panzavolta, N. Roveri and K. Rubini. Stabilization of gelatin films by crosslinking with genipin. Biomaterials 23: 4827-4832, 2002.
4. Chimene D., K. K. Lennox, R. R. Kaunas and A. K. Gaharwar. Advanced bioinks for 3D printing: A materials science perspective. Annals of biomedical engineering 44: 2090-2102, 2016.
5. Choi Y.-J., H.-G. Yi, S.-W. Kim and D.-W. Cho. 3D Cell Printed Tissue Analogues: A New Platform for Theranostics. Theranostics 7: 3118, 2017.
6. Song S. J., J. Choi, Y. D. Park, S. Hong, J. J. Lee, C. B. Ahn, H. Choi and K. Sun. Sodium Alginate Hydrogel-Based Bioprinting Using a Novel Multinozzle Bioprinting System. Artificial organs 35: 1132-1136, 2011.
7. Anil Kumar S., S. C. Allen, N. Tasnim, T. Akter, S. Park, A. Kumar, M. Chattopadhyay, Y. Ito, J. Suggs and B. Joddar. The applicability of furfuryl-gelatin as a novel bioink for tissue engineering applications. Journal of Biomedical Materials Research Part B: Applied Biomaterials 2018.
8. Jia J., D. J. Richards, S. Pollard, Y. Tan, J. Rodriguez, R. P. Visconti, T. C. Trusk, M. J. Yost, H. Yao and R. R. Markwald. Engineering alginate as bioink for bioprinting. Acta Biomaterialia 10: 4323-4331, 2014.
9. Zhang Q., X. Yang, P. Li, G. Huang, S. Feng, C. Shen, B. Han, X. Zhang, F. Jin and F. Xu. Bioinspired engineering of honeycomb structure–Using nature to inspire human innovation. Progress in Materials Science 74: 332-400, 2015.
10. Nair K., M. Gandhi, S. Khalil, K. C. Yan, M. Marcolongo, K. Barbee and W. Sun. Characterization of cell viability during bioprinting processes. Biotechnology journal 4: 1168-1177, 2009.
11. Begum J., W. Day, C. Henderson, S. Purewal, J. Cerveira, H. Summers, P. Rees, D. Davies and A. Filby. A method for evaluating the use of fluorescent dyes to track proliferation in cell lines by dye dilution. Cytometry Part A 83: 1085-1095, 2013.
12. Filby A., E. Perucha, H. Summers, P. Rees, P. Chana, S. Heck, G. M. Lord and D. Davies. An imaging flow cytometric method for measuring cell division history and molecular symmetry during mitosis. Cytometry Part A 79: 496-506, 2011.
13. Joddar B., E. Garcia, A. Casas and C. M. Stewart. Development of functionalized multi-walled carbon-nanotube-based alginate hydrogels for enabling biomimetic technologies. Scientific reports 6: 2016.
14. Pati F., J.-H. Shim, J.-S. Lee and D.-W. Cho. 3D printing of cell-laden constructs for heterogeneous tissue regeneration. Manufacturing Letters 1: 49-53, 2013.
15. Park S.-h., S.-y. Seo, H.-n. Na, K.-i. Kim, J.-w. Lee, H.-d. Woo, J.-h. Lee, H.-k. Seok, J.-g. Lee and S.-i. Chung. Preparation of a visible light-reactive low molecular-O-carboxymethyl chitosan (LM-O-CMCS) derivative and applicability as an anti-adhesion agent. Macromolecular research 19: 921, 2011.
16. Park S. H., S. Y. Seo, J. H. Kang, Y. Ito and T. I. Son. Preparation of photocured azidophenyl-fish gelatin and its capturing of human epidermal growth factor on titanium plate. Journal of Applied

456 Polymer Science 127: 154-160, 2013.
457 17. Mazaki T., Y. Shiozaki, K. Yamane, A. Yoshida, M. Nakamura, Y. Yoshida, D. Zhou, T. Kitajima,
458 M. Tanaka and Y. Ito. A novel, visible light-induced, rapidly cross-linkable gelatin scaffold for
459 osteochondral tissue engineering. Scientific reports 4: 4457, 2014.
460 18. Son T. I., M. Sakuragi, S. Takahashi, S. Obuse, J. Kang, M. Fujishiro, H. Matsushita, J. Gong, S.
461 Shimizu, Y. Tajima, Y. Yoshida, K. Suzuki, T. Yamamoto, M. Nakamura and Y. Ito. Visible light-
462 induced crosslinkable gelatin. Acta Biomaterialia 6: 4005-4010, 2010.
463 19. Stowers R. S., S. C. Allen and L. J. Suggs. Dynamic phototuning of 3D hydrogel stiffness.
464 Proceedings of the National Academy of Sciences 112: 1953-1958, 2015.
465 20. Gaetani R., D. A. Feyen, V. Verhage, R. Slaats, E. Messina, K. L. Christman, A. Giacomello, P. A.
466 Doevendans and J. P. Sluijter. Epicardial application of cardiac progenitor cells in a 3D-printed
467 gelatin/hyaluronic acid patch preserves cardiac function after myocardial infarction. Biomaterials
468 61: 339-348, 2015.
469 21. Ornelas A., K. N. Williams, K. Hatch, A. Paez, A. C. Aguilar, C. C. Ellis, N. Tasnim, S. Ray, C.
470 Dirk and T. Boland. Synthesis and Characterization of a Photocleavable Collagen-Like Peptide.
471 Organic & biomolecular chemistry 2018.
472 22. Torrado A. R. and D. A. Roberson. Failure Analysis and Anisotropy Evaluation of 3D-Printed
473 Tensile Test Specimens of Different Geometries and Print Raster Patterns. Journal of Failure
474 Analysis and Prevention 16: 154-164, 2016.